2007

Up-regulation of tau, a brain microtubule-associated protein, in lens cortical fractions of aged αA-, αB-, and αA/B-crystallin knockout mice

Fang Bai
Washington University School of Medicine in St. Louis

Jing-hua Xi
Washington University School of Medicine in St. Louis

Usha P. Andley
Washington University School of Medicine in St. Louis

Molecular Vision 2007; 13:1589-600 <http://www.molvis.org/molvis/v13/a177/>
Received 17 July 2007 | Accepted 24 August 2007 | Published 6 September 2007

Up-regulation of tau, a brain microtubule-associated protein, in lens cortical fractions of aged αA-, αB-, and αA/B-crystallin knockout mice

Fang Bai, Jing-hua Xi, Usha P. Andley

Department of Ophthalmology and Visual Sciences, and of Biochemistry and Molecular Biophysics, Washington University School of Medicine, St. Louis, MO

Purpose: α-Crystallin is expressed at high levels in the lens in a complex of αA- and αB-crystallin subunits in 3:1 molar ratios, and is known to maintain the solubility of unpolymerized tubulin and enhance the resistance of microtubules to depolymerization, but its effect on proteins classically associated with microtubule stability (microtubule associated proteins) in the lens is unknown. In the present study we examined the expression of the brain microtubule associated protein tau in lenses of α-crystallin gene knockout mice.

Methods: Quantitative RT-PCR, immunoblotting, cryo-immunoelectron microscopic and immunohistochemical methods were used to characterize the expression of tau in the lenses of $\alpha A^{-/-}$-, $\alpha B^{-/-}$-, and $\alpha A/B^{-/-}$-crystallin mice.

Results: Immunoreactivity to tau, a 45-66 kDa brain microtubule associated protein that has been best characterized in neurons and neuronal pathologies, was uniquely upregulated in lens cortical fiber cells with aging and was associated with the microtubule fraction of $\alpha A^{-/-}$-, $\alpha B^{-/-}$-, and $\alpha A/B^{-/-}$-crystallin mouse lenses, but was undetectable in wild type lenses. Quantitative RT-PCR analysis further showed an upregulation of tau transcripts in $\alpha A^{-/-}$- and $\alpha A/B^{-/-}$-crystallin lenses. Brain microtubule fractions served as a positive control for tau in these experiments. An increase in phosphorylation of tau was detected in $\alpha A^{-/-}$- and $\alpha B^{-/-}$-crystallin brain proteins.

Conclusions: Although tau aggregation and αB-crystallin expression have been shown to increase in neurodegenerative diseases, surprisingly tau expression increases in the α-crystallin knockout lenses, suggesting that αA- and αB-crystallins are potentially important regulators of tau expression in lens.

The vertebrate lens is composed of a single layer of epithelial cells on its anterior surface, which divide and differentiate in the equatorial zone, and undergo elongation, and nuclei and organelle degradation [1,2]. This orderly process continues throughout life, and is thought to be responsible for maintaining a transparent lens. The lens fiber cells have a limited ability to turnover proteins as the lens ages. α-Crystallin, a major protein of lens fiber cells, is a member of the small heat shock protein family of chaperones, and is isolated from the lens as a complex of αA- and αB-crystallin subunits in 3:1 stoichiometry [3]. The α-crystallins are expressed very early during lens development [4]. Both αA- and αB-crystallin have been shown to be expressed in tissues outside the lens including brain [5,6]. The αB-crystallin subunit is a stress-induced protein that is widely expressed in tissues outside the lens, whereas the αA-crystallin subunit is more lens-specific and is not stress inducible [7-9]. Recent work suggests that αA- and αB-crystallin play a role in development and growth by interacting with components of cellular protein degradation machinery and maintaining the cytoskeleton, thereby regulating diverse cellular processes [10-12]. αA- and αB-crystallin are thought to selectively recognize and bind to exposed surfaces of a nonnative protein, in a noncovalent interaction to inhibit irreversible aggregation [13-15]. αB-Crystallin has also been shown to participate in the degradation of misfolded proteins that cannot be converted into the native state after repeated cycling through the chaperone systems, allowing recognition of the incompletely folded protein by an E3 ubiquitin ligase and subsequent targeting of the misfolded protein for degradation by the proteasome [16,17]. The role of αB-crystallin in proteasomal targeting has also been shown during normal cellular processes, as illustrated by degradation of cyclin D1 during the cell cycle [17].

The brain microtubule associated protein tau, known to stabilize the microtubule cytoskeleton and promote microtubule assembly, is a group of 45-66 kDa proteins encoded by alternative splicing of a single gene [18]. There are six predominant tau isoforms in human brain containing 352-441 amino acids [19]. The tau proteins are unstructured in solution but bind in an ordered conformation along the microtubule protofilaments to stabilize and/or strengthen interactions between adjacent protofilament and increase microtubule integrity [20]. Aggregation of tau into paired helical filaments via hyperphosphorylation is the main component of neurofibrillary tangles found in the brains of Alzheimer disease (AD) patients [21-23]. Tau is thought to be associated with the primary pathology and neuronal damage in tauopathies

Correspondence to: Usha P. Andley, Ph.D., Department of Ophthalmology and Visual Sciences, Washington University School of Medicine, 660 S. Euclid Avenue, Campus Box 8096, St. Louis, MO, 63110; Phone: (314) 362-7167; FAX: (314) 362-3638; email andley@vision.wustl.edu

like frontotemporal dementia (FTDP) [24-26]. The molecular chaperone/stress-inducible small heat shock protein αB-crystallin is known to be upregulated in astrocytes associated with senile plaques and cerebral amyloid angiopathy in AD [27,28]. αB-Crystallin is also associated with Lewy body disease, Parkinson disease, multiple sclerosis, FTDP and other neurodegenerative disorders [28-30]. The specific role of αB-crystallin in these disorders is unknown. Investigators have detected an early defining feature of Alzheimer disease, the Aβ peptides in the cytosol of the lens fiber cells, and suggested that the Aβ-mediated aggregation of lens proteins contributes to increased light scattering in the lens [31,32]. Indeed, several studies suggest protein-protein interactions between αB-crystallin and Aβ [33,34]. αB-Crystallin has also been shown to inhibit the aggregation of small Aβ peptides into mature fibrils in vitro [35]. Furthermore, studies by Frederikse et al. [36] on microtubules and kinesin based transport in the lens suggest several fundamental parallels between lens and neuronal vesicle trafficking and cell biology, and suggest that Aβ-related vesicle trafficking disease mechanisms may be shared by lens and brain.

The microtubule cytoskeleton is a very dynamic network that plays a crucial role in key biologic processes such as cell division and intracellular traffic [37]. Microtubule dynamic instability and functions are regulated by microtubule-associated proteins (MAPs). αB-Crystallin enhances microtubule resistance to depolymerization, and maintains tubulin levels in vivo in muscle cells [38,39]. Our previous studies with αA-, αB- and αA/B-crystallin gene knockout mice suggested that the depletion of these chaperones is associated with changes in cell cycle parameters, and more specifically, a microtubule instability phenotype [40-43]. We therefore investigated the expression of the brain MAP tau, known to enhance microtubule stability, in microtubule fractions from αA- and αB-crystallin gene knockout mice in the current work. Surprisingly, in the αA- and αB-crystallin gene knockout mice we found that the tau is uniquely upregulated in the differentiated lens cortical fiber cells, which have a limited ability to turnover protein as the lens ages. Our results demonstrate that the lens is an important organ that can capture some of the systemic pathology involved in protein aggregation disorders that affect the brain, and suggest that the α-crystallin knockout mice may be a good model to study disease mechanisms involving protein aggregation in the brain.

METHODS

Animals and tissues: Wild type and $\alpha A^{-/-}$-, $\alpha B^{-/-}$-, and $\alpha A/B^{-/-}$- knockout mice were used in this study. Wild type mice were the 129SvEv strain from Taconic Farms (Hudson, New York). The crystallin knockout mice $\alpha A^{-/-}$-, αB/HSPB2$^{-/-}$- (termed $\alpha B^{-/-}$- in this study) and αA/αB/HSPB2$^{-/-}$- (termed $\alpha A/B^{-/-}$- in this study) were kindly provided by E. Wawrousek (National Eye Institute, NIH, Bethesda, MD) [44,45]. αB-Crystallin has also been termed HSPB5 [46]. Mice were inbred and all animal protocols were in accordance with the institutional policy on the use of animals in research [40,41]. Mice were used at 1 to 12 months of age. At the appropriate age, animals were killed by CO_2 inhalation. Whole eyes were dissected, fixed and sectioned for immunofluorescent detection of tau. Whole lenses were dissected and epithelial and cortical fractions (Figure 1A) were isolated under a microscope, and were used to prepare microtubules and microtubule associated proteins as described previously [42,43]. Lens cortical fractions were used for RNA isolation. Brains collected from the mice of each genotype were also used.

Antibodies: The following tau antibodies were used for immunoblot, immunofluorescence and cryo-immuno electron microscopic (em) analysis: (1) KAM- MA305 (Stressgen, Ann

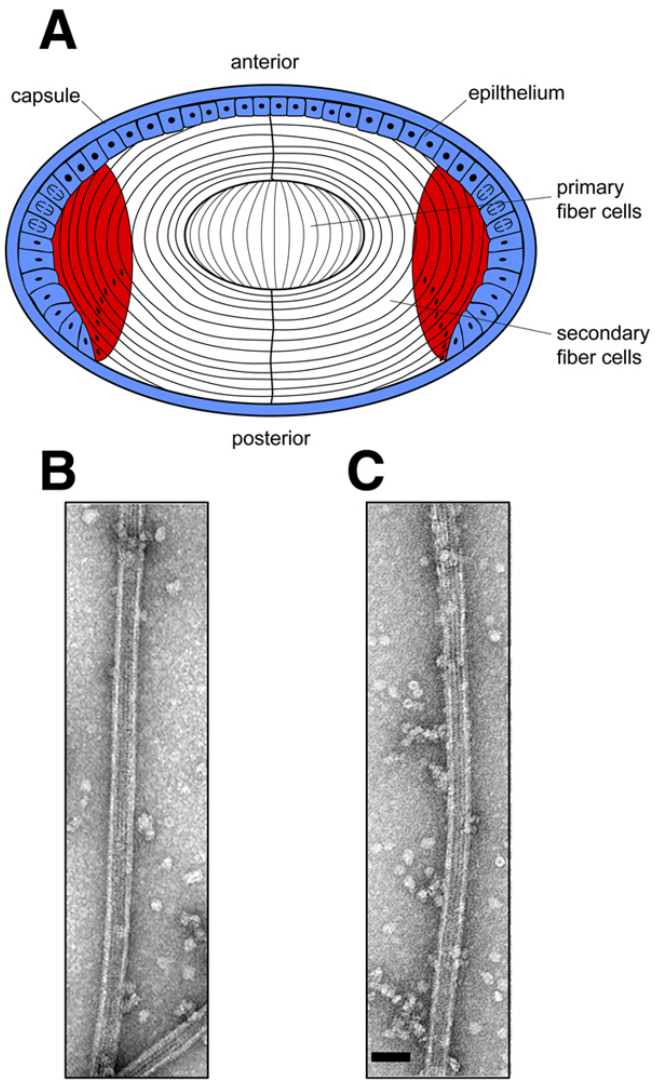

Figure 1. Preparation of microtubule associated proteins. **A**: Dissection of mouse lens epithelial and cortical fractions used for the isolation of microtubule associated proteins (MAPs). Wild type, $\alpha A^{-/-}$-, $\alpha B^{-/-}$-, and $\alpha A/B^{-/-}$- lenses were dissected into epithelial (blue) and cortical fiber cell (red) fractions. Microtubules were reconstituted from lens cortical fiber cell lysates and MAPs were extracted as described under Experimental Procedures. **B** and **C**: Electron micrographs of mouse lens cortical fiber microtubules that were used to dissociate the MAPs. Microtubules were negatively stained and examined. **B** shows wild type microtubules and **C** shows $\alpha B^{-/-}$- microtubules. The scale bar is equal to 50 nm.

Arbor, MI) at 1:1000 dilution for immunoblotting, and 1:100 for cryo-immuno em and immunofluorescence; (2) AT8 antibody to PHF-tau (Pierce, Rockford, IL) at 1:40 dilution for immunoblotting and immunofluorescence, and 1:5 for cryoimmuno electron microscopy [47]; (3) TAU-5 (Lab Vision, Fremont, CA) at 1:200 dilution for immunoblotting and 1:5 for cryoimmuno electron microscopy [48-50]; (4) pS422 (Biosource, Carlsbad, CA) at 1:1000 dilution [48].

Quantitative reverse transcriptase polymerase chain reaction (RT-PCR): Total RNA from wild type and knockout ($\alpha A^{-/-}$-, $\alpha B^{-/-}$-, and $\alpha A/B^{-/-}$-) was isolated from mouse lens cortical fractions and mouse brain fractions by the Qiagen kit. One μg of total RNA was used for each sample to prepare cDNA. The RNA was treated with DNase and first strand cDNA synthesis was performed using a kit from Invitrogen using Oligo(dT) as primer. Primers were designed and synthesized by Integrated DNA Technologies (Coralville, IA). Their concentrations optimized using the manufacturer's recommendations. The forward and reverse primers used for mouse tau gene are shown in Figure 2. To optimize the primers, reverse-transcriptase polymerase chain reaction (RT-PCR) was performed and products were run on 1.5% agarose gels to ascertain that a single band of the correct size was obtained. Real time-PCR was performed using a supermix containing the fluorescent dye SYBR green (BioRad, Hercules, CA) as described previously [51]. The increase in fluorescence was detected using the iCycler (BioRad). The relative quantification of tau gene expression was performed using the standard curve method according to manufacturer's instructions (BioRad). For comparison between wild type and knockout samples, a standard curve of cycle thresholds for several serial dilutions of RNA sample was established and then used to calculate the relative abundance levels of mRNA (mRNA). The expression level of each tau mRNA was determined relative to GAPDH of the same sample. All RT-PCR reactions were performed in triplicate, and three independent experiments were performed on lens and brain samples.

Isolation of microtubule associated proteins: Microtubules were reconstituted from freshly dissected mouse lens epithelial and cortical fractions (Figure 1) [42,52]. Briefly, lens cortical fraction pooled from 16 to 20 mouse lenses was homogenized in 100 μl PME buffer (80 mM PIPES, 1 mM $MgCl_2$, 1 mM EGTA, pH 6.8) at 4 °C, followed by centrifugation at 30,000g for 15 min and the resulting supernatants were centrifuged at 100,000g for 60 min in a Beckman Optima TLX ultracentrifuge. Taxol (20 μM) and GTP (1 mM) were added to the supernatants, and incubated for 15 min at 37 °C, followed by centrifugation at 30,000 g for 15 min at 37 °C through a sucrose cushion to pellet the microtubules. Microtubule associated proteins were extracted by washing the pellets in 0.35 M NaCl, and centrifugation at 30,000g for 25 min. This procedure has been shown to extract the MAPs in the supernatant [52]. Microtubules were examined by electron microscopy on negatively stained microtubule pellets as described previously [42]. To analyze tau expression in the brain, wild type and $\alpha A^{-/-}$-, $\alpha B^{-/-}$-, or $\alpha A/B^{-/-}$- brains were homogenized in PME

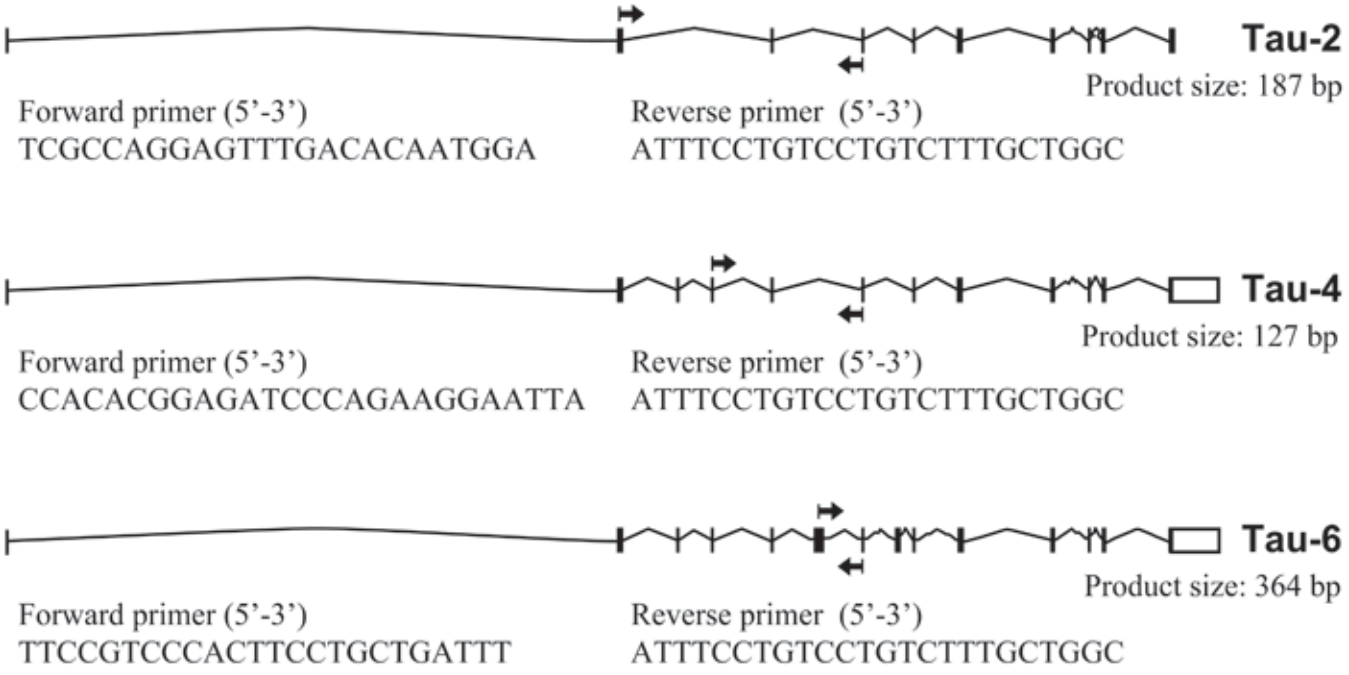

Figure 2. Transcripts for mouse tau. The three major tau transcripts were designated Tau-2, Tau-4, and Tau-6. The Ensembl transcript ENSMUST00000018555 was used to design gene-specific primers. Exons are indicated by vertical lines. Horizontal arrows indicate the sites for sequence-specific primers. The following nucleotides correspond to the primers: Exon 2 forward primer: nucleotide +12 to +35; Exon 4 forward primer: nucleotide +431 to +456; Exon 6 forward primer: nucleotide +905 to +928; Exon 7 reverse primer: antisense of nucleotide +1268 to +1245.

buffer and microtubule associated proteins were isolated as described above for lens tissue.

Gel electrophoresis and immunoblot analysis: Supernatants containing MAPs were analyzed by SDS-PAGE and immunoblotting, using several commercially available antibodies to tau described above. Proteins were separated using SDS-PAGE as described previously [42,53,54]. Samples were heated to 95 °C in sample buffer for SDS-PAGE. In experiments on brain tissue, better visualization of proteins in immunoblots was obtained when temperature was lowered to 85 °C. To examine the expression of tau in MAP fractions of wild type and knockout lens cortical fiber cells, equal amount

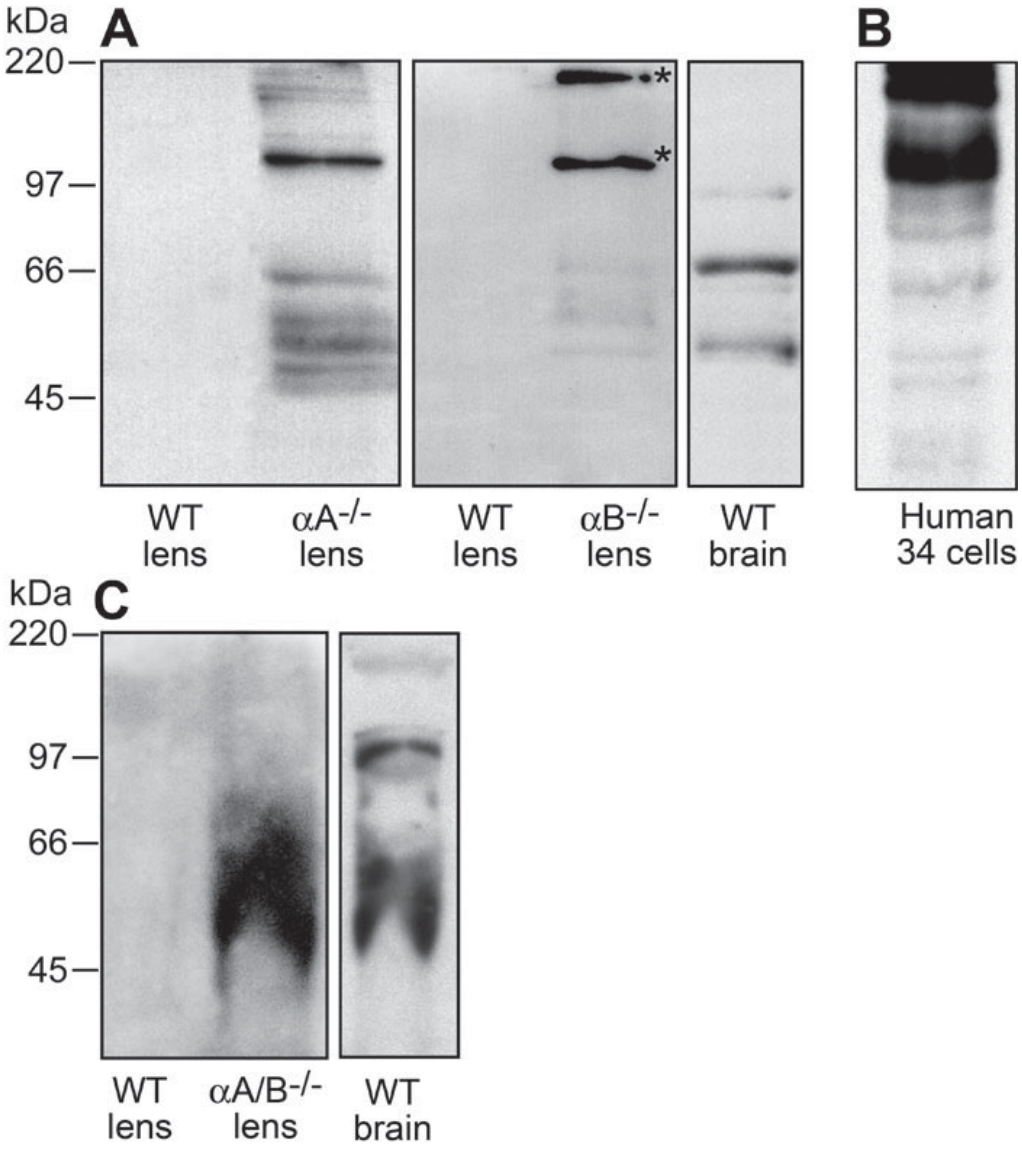

Figure 3. Immunoblot analysis of tau in mouse lens. Lens cortical fiber cell MAPs from 8-month-old wild type, $\alpha A^{-/-}$- and $\alpha B^{-/-}$- mice were prepared and the proteins were separated by SDS-PAGE. Tissue from 16 to 20 lenses was pooled for each preparation. Samples were heated to 95 °C in SDS-PAGE sample buffer to detect tau in lens samples. Immunoblot analysis was performed with the monoclonal antibody KAM-MA305 to full length brain tau protein and the Tau-5 antibody which reacts with nonphosphorylated as well as phosphorylated forms of tau. **A**: Antibody used was KAM-MA305 to full length brain tau. Left panel, Wild type (WT) and $\alpha A^{-/-}$- MAPs. Tau was undetectable in the wild type lenses, but tau immunoreactive proteins were detected in the 45-66 kDa range in the $\alpha A^{-/-}$- and $\alpha B^{-/-}$- lens fractions. Note that the $\alpha A^{-/-}$- tau immunoreactive bands included a prominent 100 kDa band; middle panel, WT and $\alpha B^{-/-}$- MAPs. Tau immunoreactivity was undetectable in the wild type MAPs from cortical fiber cells, but higher molecular weight crosslinked bands (asterisks) crossreacted with the antibody in the $\alpha B^{-/-}$- MAPs. Right panel, Microtubule associated proteins were isolated from 3-month-old mouse brains and analyzed by SDS-PAGE and immunoblotting. Note that the major immunoreactive bands were detected at 45-66 kDa, whereas minor bands were detected at about 100 kDa. **B**: Human cells-34 lysates were analyzed with the KAM-MA305 antibody. Tau immunoreactive bands at about 100 and 200 kDa bands were prominent in these cells. **C**: Antibody used was the Tau-5 antibody which recognizes both nonphosphorylated and phosphorylated forms of tau; left panel, Immunoreactivity of wild type and $\alpha A/B^{-/-}$- lens fractions. Although no immunoreactive bands were detected in the wild type lens, a broad band was observed in the $\alpha A/B^{-/-}$- lens; right panel, wild type brain fractions run on the same gel with a similar broad band showing immunoreactivity to this antibody.

of total protein was loaded from each sample. Immune complexes were detected using a horseradish peroxidase labeled secondary antibody and luminol (Santa Cruz Biotechnology, Santa Cruz, CA). The detected proteins were quantified with an Alpha Innotech photoimaging system (San Leandro, CA) [42].

Immunolabeling and confocal microscopy of the microtubule associated protein tau: To examine tau immunolabeling in the lens, wild type and α-crystallin knockout eyes were fixed and mounted in glycol methacrylate [41,43]. Three micron sections were cut in the mid-sagittal plane [41]. Nonspecific binding was blocked by incubation with normal goat serum for 30 min. To visualize the distribution of tau, tissues were incubated overnight with a 1:100 dilution of an antibody to tau, and an Alexa-568-conjugated secondary antibody (1:200). Immunofluorescence and confocal microscopy were performed in the red channel of a Zeiss 510 confocal microscope. Differential interference contrast (DIC) was used to examine morphology in the blue channel of the confocal microscope [41].

Cryoimmuno electron microscopic analysis: Lens sections were examined by cryo-immuno electron microscopy. Sections (50-80 nm) were treated with primary antibodies to tau KAM-MA305 (Stressgen) and Tau-5 (Laboratory Vision) and anti-mouse IgG conjugated with 18 nm gold particles as secondary antibody (Sigma, St. Louis, MO). Specimens were stained with uranyl acetate and examined in a 1200EX transmission electron microscope as described previously [55,56].

UVB irradiation of lenses: Wild type 129SvEv mice were irradiated with FS20 UVB lamps emitting 290-320 nm radiation (maximum output at 310 nm) at a fluence rate of 7.8 W/m^2 for 60 min, with a total fluence of 28 kJ/m^2 at the cornea [57]. Twenty-four h later, mice were sacrificed and eyes were dissected and sectioned. Tau expression was visualized in control and UVB-exposed lenses by immunofluorescence analysis using antibodies to tau, and sectioned were examined by confocal microscopy.

RESULTS

Previous studies on gene knockout models of αA- and αB-crystallin suggested a decrease in lens microtubule stability [42]. As a first step to verify this observation, we examined the expression of the tau, a brain microtubule-stabilizing protein, in the lens. Lens cortical fractions were dissected (Figure 1A) and microtubule fractions were isolated (Figure 1B,C). More clusters appear to be associated with $\alpha B^{-/-}$- microtubules than wild type as described previously [42].

Expression of tau protein in lens fiber cells: Lens microtubule fractions containing microtubules and MAPs were examined for tau protein expression by immunoblotting using an antibody made against full-length brain tau protein. Tau immunoreactivity was undetectable in the wild type lens MAP fractions. Tau immunoreactive bands at the expected mobilities were observed in $\alpha A^{-/-}$- lens cortical fiber cells of mice 6 months of age and older (Figure 3) A distinct band of slower electrophoretic mobility corresponding to a molecular mass of 100 kDa was also detected in the $\alpha A^{-/-}$- lens fractions. In addition, a group of significantly weaker bands of about 200 kDa were detected in the $\alpha A^{-/-}$- lens fractions (Figure 3). The $\alpha B^{-/-}$- lens fractions also demonstrated immunoreactivity to the tau antibody in the 45-66 kDa range. Two bands having lower electrophoretic mobilities, and about 100 kDa and 200 kDa mass crossreacted with the tau antibody in the $\alpha B^{-/-}$- lens fractions. We used brain MAP preparations as positive control for the antibody against tau that was run together with the lens samples for comparison (Figure 3). Mouse brain MAPs showed strong tau immunoreactivity with distinct 45-66 kDa proteins, suggesting that the 45-66 kDa bands in the lens samples are unlikely to be nonspecific artifacts that cross react with the tau antibody. In addition, the brain fractions expressed a weaker tau immunoreactive band at 100 kDa. We also used a positive antibody control, human cells-34. These cells are known to produce tau in abundance. Immunoreactive bands to tau were observed both in the 45-66 kDa as well

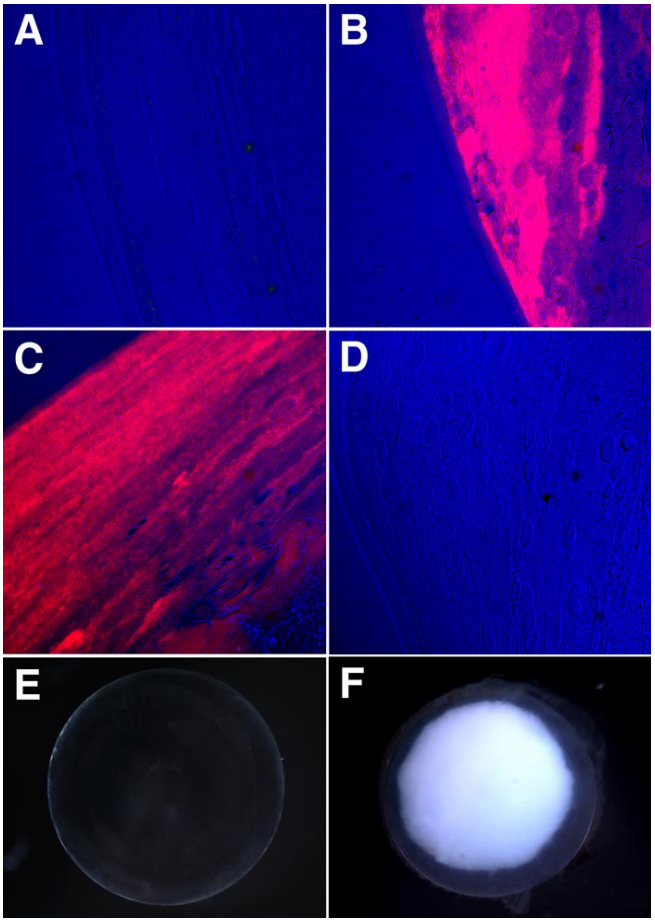

Figure 4. Immunofluorescence analysis of tau in the lens. Anti-tau immunostaining in lens sections from 6-month-old-mice. Red=tau; blue=DIC. **A**: Wild type lens. **B**: $\alpha A/B^{-/-}$- lens. **C**: $\alpha B^{-/-}$- lens. **D**: Absence of immunofluorescence in the lens specimen of a 6-month-old $\alpha A/B^{-/-}$- lens probed with non-immune mouse IgG. The scale bar is equal to 25 μm. **E**: Dark field image of a 6-month-old wild type mouse lens. **F**: Dark field image of a 6-month-old $\alpha A/B^{-/-}$- lens. Note that the opacity occupies three quarters of the lens. Note also that the outer cortex of the $\alpha A/B^{-/-}$- lens remains relatively clear.

as about 100 and 200 kDa molecular mass range. To further establish that the proteins detected with the KAM antibody were indeed tau, a previously well characterized tau antibody (Tau-5) against brain tau was also used. This antibody which detects both non-phosphorylated and phosphorylated tau proteins detected a strong broad band in the 45-66 kDa range in the αA/B$^{-/-}$- but not the wild type lens, and in the wild type brain (Figure 3C). Similar results were obtained with lens fractions of αA$^{-/-}$- and αB$^{-/-}$- lenses (data not shown).

The distribution of tau immunoreactive proteins was examined by immunofluorecence and confocal microscopy. Lens sections from wild type and αA/B$^{-/-}$- mice were treated with an antibody to tau and examined by confocal microscopy. Figure 4 shows a strong increase in immunofluorescence of the αB$^{-/-}$- lenses as compared with wild type lenses (Figure 4A-C). Figure 4C also shows that the distribution of tau in the cortical fiber cells of αB$^{-/-}$- lenses appears to follow the lens fiber cell length. Replacement of the primary antibody with a non-immune mouse IgG and normal rabbit serum did not result in immunofluorescence staining (Figure 4D). These data suggest that our results are not attributable to non-specific staining artifact. Although tau immunoreactivity was observed in newly formed cortical fiber cells (Figure 4B,C), it was not detectable in the inner nuclear fibers, where where lenses of αA/B$^{-/-}$- mice develop nuclear cataract (Figure 4E,F). To further confirm the increase in expression of tau in the αB$^{-/-}$- mouse lenses, cryo-immunoelectron microscopy was employed. Figure 5A,B show cryo-immunolabeling of tau in wild type and αB$^{-/-}$- mouse lens cortical fiber cells, respectively. Very sparse background labeling was observed in the wild type lens cortical fiber cells with the KAM antibody. In contrast, the αB$^{-/-}$- lens cortical fibers showed abundant labeling, with clusters of immunogold particles in electron dense regions. Figure 5C,D show the immunolabeling of lens cortical fibers with the Tau-5 antibody. A vast increase in labeling was observed in the αB$^{-/-}$- lenses whereas wild type lenses showed no labeling. These data confirm the upregulation of tau in the αB$^{-/-}$- lens cortical fiber cells.

A developmental time course for the appearance of tau immunoreactive proteins in mouse lens cortical fiber cells was performed. Figure 6 shows the effect of mouse age on expression of tau immunoreactivity in αA$^{-/-}$-, αB$^{-/-}$-, and αA/B$^{-/-}$- lenses. In lenses of mice less than 4 months old, no tau isoforms (45-66 kDa) were detectable by immunoblot analysis. Tau expression stabilized in lens fractions derived from mice older than 6 months of age. These results indicate that the change in tau immunoreactivity in lens cortical fiber cells of α-crystallin gene knockout mice occurs around six months of age. A parallel study in lens epithelial cells with age showed that the expression of tau immunoreactivity was very weak in wild type or αA$^{-/-}$-, αB$^{-/-}$-, and αA/B$^{-/-}$- epithelial fractions (data not shown). Taken together, the immunoblot, immunofluorescence and cryo immunoelectron microscopic analysis indicated that the loss of chaperones αA- and αB-crystallins resulted in enhancement of tau immunoreactive proteins in the differentiated lens cortical fiber cells.

Transcriptional activity of tau in the lens: We next examined the expression of tau transcripts in the lenses of wild type and α-crystallin gene knockout mice. Tau is encoded via the transcription of a single gene by alternative splicing [18,23]. We designed primers specific to sequences in tau gene encoding the major tau peptides (Figure 2). Transcriptional activity

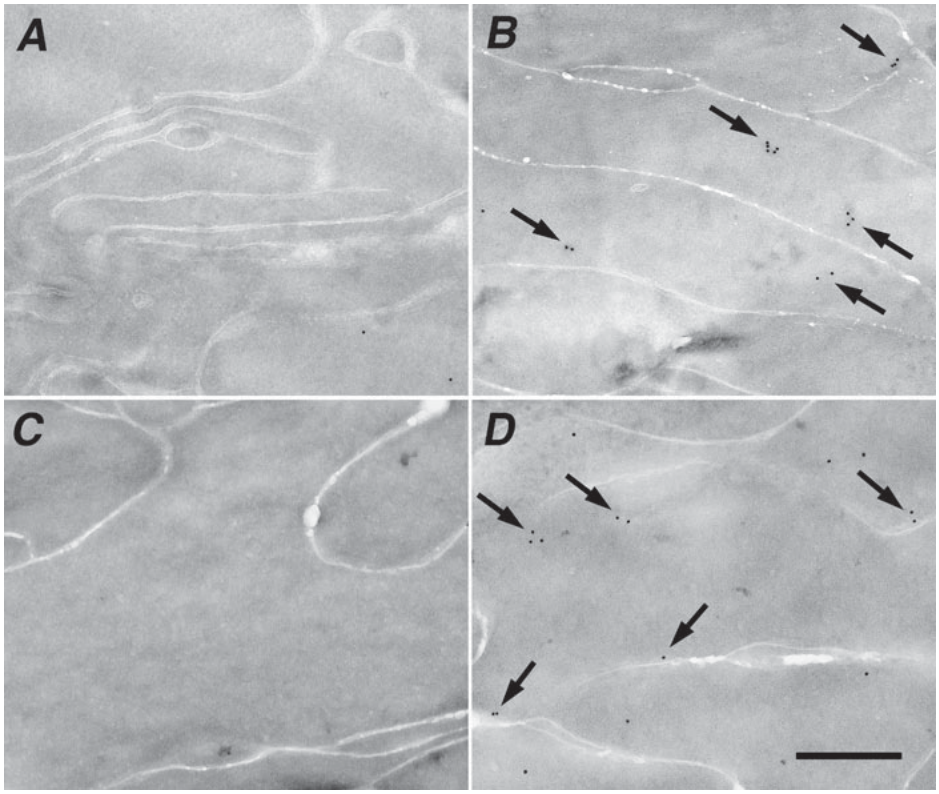

Figure 5. Cryo-immuno electron microscopy of tau in the lens. Anti-tau cryo-immuno electron microscopy in lens sections from 8-month-old mice with the antibody KAM-MA305 (**A** and **B**) or Tau-5 (**C** and **D**). **A**: Absence of cryo-immuno labeling in the lens cortical fiber cells of an 8-month-old wild type mouse. **B**: αB$^{-/-}$- lens shows ample immunostaining with the tau antibody KAM-MA305, with clusters of immunogold particles in electron dense areas of the cells (arrows). **C**: Absence of immunostaining in 7-month-old wild type lens. **D**: αB$^{-/-}$- lens shows ample immunostaining with the tau-5 antibody, with numerous immunogold particles in lens fiber cells (arrows). All images are shown at the same magnification. The scale bar is equal to 0.5 μm.

of tau gene in the lens was confirmed by RT-PCR (Figure 7). A 187 bp fragment was amplified using a pair of gene-specific primers designed to anneal to sequences associated with the Tau-2 transcript (Figure 2). This was the major tau transcript detected in the lens, and corresponded to expression of the smallest mouse tau peptide with 372 amino acid residues (Figure 2). Primers specific to the alternatively spliced Tau-4 transcript encoding the medium-length (432 residues) tau protein amplified a 127 bp PCR product in the brain (Figure 8) but not in the lens (Figure 7), suggesting that this transcript is not expressed in the lens. Similarly, a 364 bp PCR product was amplified from primers sequences designed to amplify the transcript encoding the longest tau peptide (733 residues) in the lens (Figure 7). Quantitative RT-PCR reactions were performed to assess the effect of αA- and αB-crystallin gene knockout on tau gene expression. GAPDH gene expression was used as a control. This analysis confirmed the expression of the Tau-2 transcript in the wild type lenses, and showed that this transcript was uniquely upregulated by 2.5 fold in the $\alpha A^{-/-}$- and a nearly fivefold in $\alpha A/B^{-/-}$- lenses, but not in $\alpha B^{-/-}$- lenses (Figure 7B). In contrast, the Tau-4 transcript was undetectable in lenses of any genotype. Although the Tau-6 transcript encoding the largest tau peptide was undetectable in the wild type and $\alpha B^{-/-}$- lenses, it was strongly upregulated in the $\alpha A^{-/-}$- and $\alpha A/B^{-/-}$- lenses. However, the relative abundance of the Tau-6 transcript was one tenth of the Tau-2 transcript in the $\alpha A^{-/-}$- and $\alpha A/B^{-/-}$- lenses. Tau transcripts were also examined in the lenses of 1 month old mice (data not shown). The tau transcripts were expressed at one fourth the levels in young (1 month old) as compared with old (6 months old) mice. The ratio of Tau-2/GAPDH transcripts was 0.3±0.05 in young lenses, increasing to 1.44±0.26 in 6 month old lenses.

Expression of tau in mouse brains: To ascertain unequivocally that tau is indeed expressed in the lens cortex, we conducted parallel studies on tau transcripts and protein expression in wild type, $\alpha A^{-/-}$-, $\alpha B^{-/-}$-, and $\alpha A/B^{-/-}$- mouse brains. This analysis is particularly relevant because αA- and αB-crystallin are also expressed at low levels in brain [5,6]. RT-

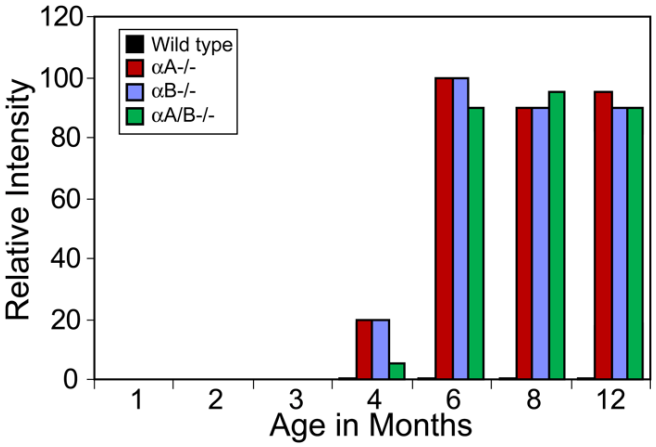

Figure 6. Effect of age on tau expression in mouse lens. Microtubule-associated proteins were isolated from cortical fiber cells of 1- to 12-month-old mice. Lenses (16-20) from each of wild type (WT), $\alpha A^{-/-}$-, $\alpha B^{-/-}$-, and $\alpha A/B^{-/-}$- mice were pooled at every age. Proteins were analyzed by immunoblotting with KAM-305 antibody to full length brain tau, and quantified by densitometric analysis. WT (black bars); $\alpha A^{-/-}$- (red bars); $\alpha B^{-/-}$- (blue bars); $\alpha A/B^{-/-}$-, (green bars).

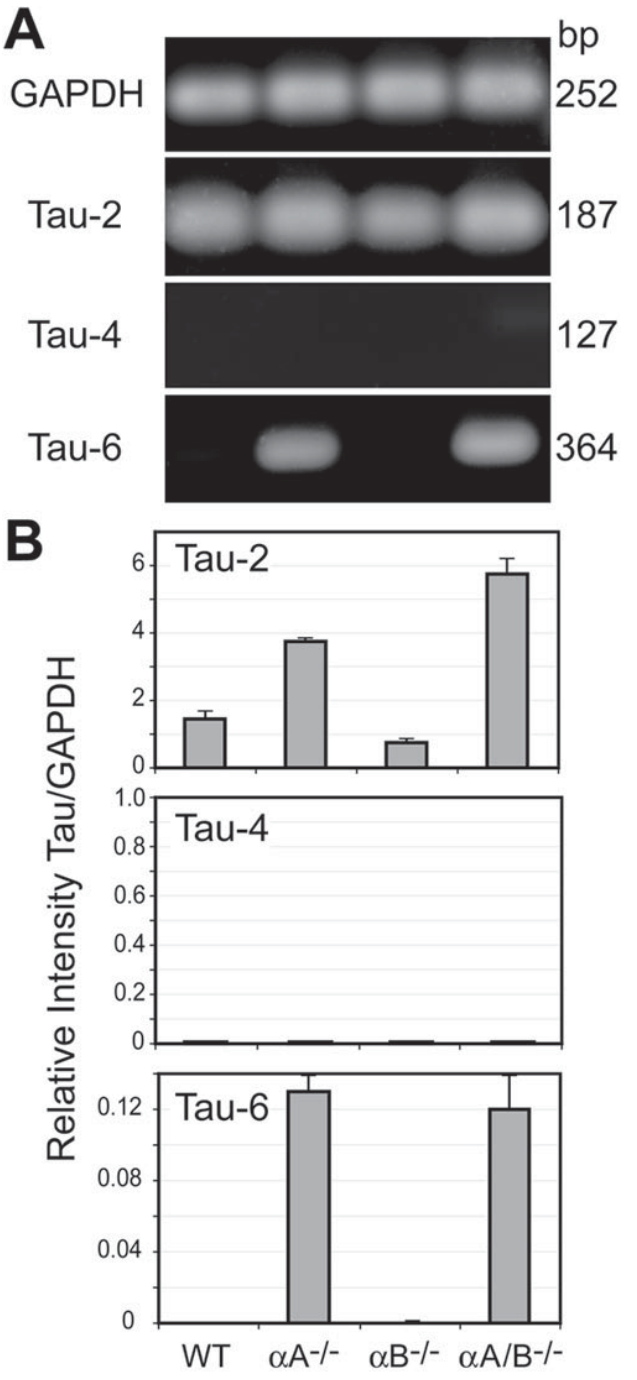

Figure 7. Quantitative RT-PCR analysis for tau transcripts in the lens. **A**: Transcripts for GAPDH, Tau-2, Tau-4, and Tau-6 were amplified from wild type, $\alpha A^{-/-}$-, $\alpha B^{-/-}$-, and $\alpha A/B^{-/-}$- lenses using the indicated primers. The primers for mouse GAPDH were: forward primer, AAG GTG AAG GTC GGA GTC AAC G, and reverse primer, GCT CCT GGA AGA TGG TGA TGG; product size, 252 bp. **B**: Quantitative RT-PCR analysis was performed. Data are representative of three independent experiments.

PCR analysis using mouse tau gene primers showed the expression of all three tau transcripts in brain (Figure 8A). The relative expression of tau transcript encoding the smallest tau peptide was 10 fold higher in the brain as compared with lenses of wild type mice. The ratio of tau-2/GAPDH was 11.2±1.7 in wild type brains as compared with 1.44±0.26 in the wild type lenses. Furthermore, in contrast to the enhanced expression of tau transcripts in αA$^{-/-}$- and αA/B$^{-/-}$- lenses as compared with wild type, quantitative RT-PCR showed that there was no significant upregulation of tau transcripts in the brains of αA$^{-/-}$- and αB$^{-/-}$- mice (Figure 8B). αA/B$^{-/-}$- brains, unlike αA$^{-/-}$- or αB$^{-/-}$- brains showed a marked reduction in the tau transcripts (Figure 8B). We next analyzed the effect of gene knockout of αA- and αB-crystallin on the expression of tau protein in the brain. Immunoblot analysis of tau protein in brains from knockout mice as compared with wild types revealed changes in relative distribution of the three murine tau isoforms in αA$^{-/-}$- and αB$^{-/-}$- brains (Figure 9). This analysis was done by heating the samples to 85 °C in SDS-PAGE sample buffer to get good resolution. Using the KAM antibody to full length brain tau, tau was detected as three immunoreactive bands in the wild type brain, but the smallest peptide band was undetectable in the αA$^{-/-}$- and αB$^{-/-}$- brains (Figure 9). Analysis of brain fractions showed that the phosphorylation-dependent PHF-tau antibody AT8 recognized mainly the highest molecular mass tau peptide in wild type brain fractions (Figure 9). Quantitative analysis of the immunoblots with the PHF tau antibody AT8 showed that the intensity of the smallest peptide increased threefold in the αA$^{-/-}$- and αB$^{-/-}$- brain fractions. While some variation between the different αB$^{-/-}$- brain samples was noted, statistical analysis showed that the increase in staining of the

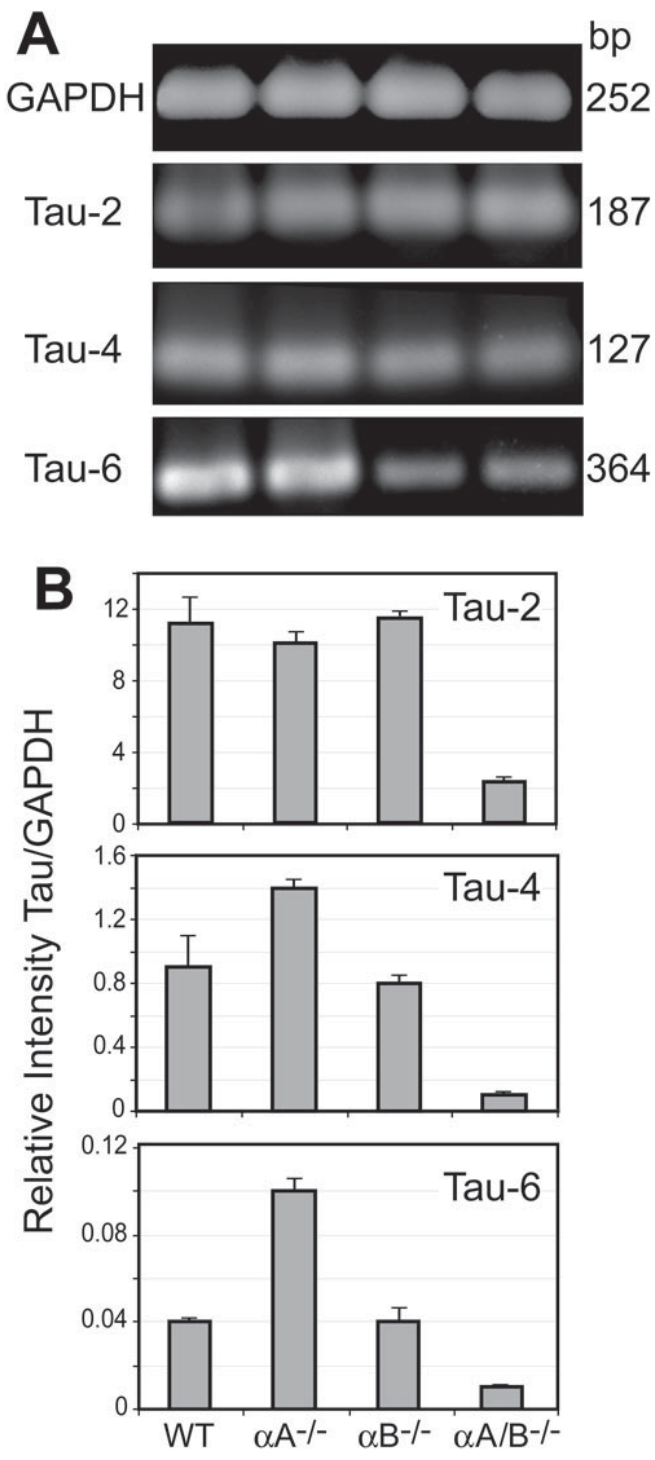

Figure 8. Quantitative RT-PCR analysis for tau transcripts in the brain. **A**: Transcripts for GAPDH, Tau-2, Tau-4, and Tau-6 were amplified from wild type, αA$^{-/-}$-, αB$^{-/-}$-, and αA/B$^{-/-}$- lenses. **B**: Quantitative RT-PCR analysis was performed. Data are representative of three independent experiments.

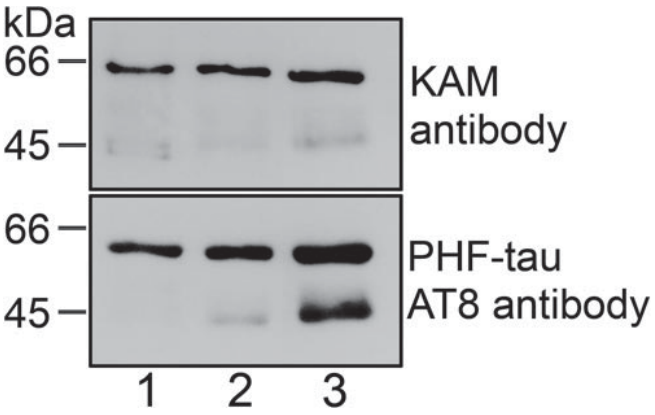

Figure 9. Immunoblot analysis of tau in mouse brain. Brain MAPs from 8-month-old wild type, αA$^{-/-}$-, and αB$^{-/-}$- mice were prepared and the proteins were separated by SDS-PAGE. Samples were heated to 85 °C in SDS-PAGE sample buffer. Ten μg proteins were applied to each lane. Immunoblot analysis was performed with the monoclonal antibody KAM-MA305 to full length brain tau protein and the PHF-tau antibody AT-8. **A**: Wild type (Lane 1), αA$^{-/-}$- (Lane 2), and αB$^{-/-}$- (Lane 3) brain MAPs. Note that three tau-immunoreactive bands were readily detected in the wild type brains with the KAM-MA305 antibody, but the smallest peptide was undetectable in the αA$^{-/-}$- and αB$^{-/-}$- brains. **B**: Wild type (Lane 1), αA$^{-/-}$- (Lane 2), and αB$^{-/-}$- (Lane 3) brain MAPs. Tau-immunoreactive bands were detected in the wild type brains with the PHF-tau AT-8 antibody. Note that the only the largest immunoreactive peptide was strongly stained in the wild type brain, but the immunoreactivity of the PHF-tau AT-8 antibody to the smaller tau peptide increased significantly in the αA$^{-/-}$- and αB$^{-/-}$- over wild type samples.

smallest peptide in the αA$^{-/-}$- and αB$^{-/-}$- brain samples was significant (p=0.01). This antibody has been shown to recognize tau protein phosphorylated at both serine 202 and threonine 205 of the longest human brain tau isoform [47]. These results suggest that gene deletion of αA- and αB-crystallin caused an increase in phosphorylation of the tau epitope Ser202/Thr205 in mouse brain. The phosphorylation-dependent antibody pS422 did not label mouse brain tau from wild type or αA$^{-/-}$- and αB$^{-/-}$- samples (data not shown). We next assessed tau staining in another mouse model for cataract by UVB irradiation of mouse lenses in vivo (Figure 10). The UVB irradiated lens showed vacuoles and opacities all over the lens surface. Positive tau staining in the UVB-irradiated lens cortex was detected by immunofluorescence analysis, suggesting that tau upregulation is not restricted to the α-crystallin knockout models.

DISCUSSION

The data presented in this investigation clearly establish the expression of the brain MAP tau in the lens. Tau immunoreactivity was detected in the pool of microtubule associated proteins derived from lens cortical fiber cell microtubules of aged in α-crystallin knockout mouse lenses. The localization of tau immunoreactivity in the microtubule fraction is important since it demonstrates that this microtubule associated protein localizes to the same cellular fraction in the lens as in the brain [52]. That tau accumulation is significant only in the cortical fiber cells and not in epithelial cells of αA- and αB-crystallin knockout lenses is attributable to the epithelial cells being able to upregulate other mechanisms that may compensate for α-crystallin, whereas cortical fiber cells cannot [58,59]. These findings expand the previously established developmentally regulated expression of cargo vesicle transport proteins, synapsins and synaptic vesicle proteins in lens [36].

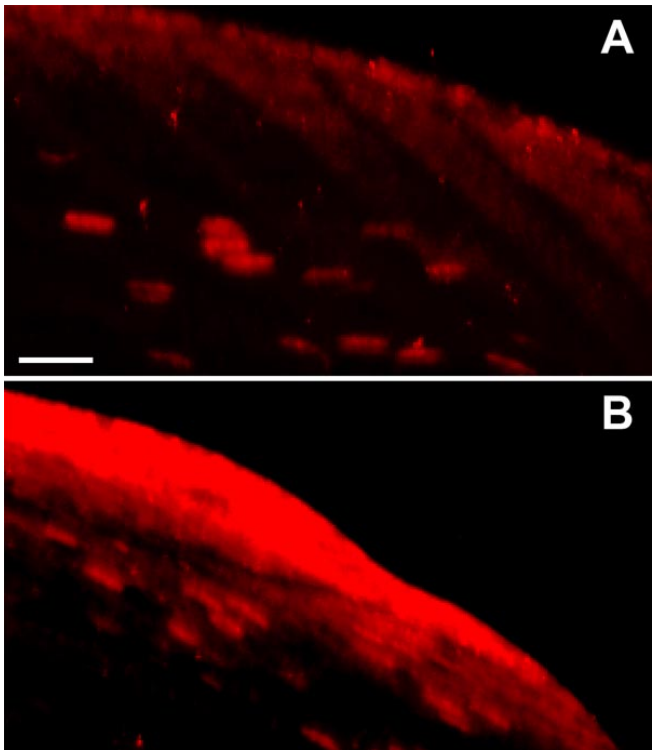

Figure 10. Expression of tau immunoreactivity in UVB mouse cataract model. Shown are the untreated lens (**A**) and the UVB-treated lens (**B**). Note the increase in lens cortical fiber cell immunostaining of tau in the UVB cataract model. Six-month-old wild type mice were exposed to 28 kJ/m^2 UVB irradiation in vivo, and the eyes were dissected and sectioned. Lens immunofluorescence was visualized using the KAM antibody to tau, which was reactive in immunoblots.

The major tau transcript (Tau-2) was expressed even in the wild type mouse lenses. The Tau-2 transcript was upregulated several fold over wild type in the αA$^{-/-}$- and αA/B$^{-/-}$- lenses. However, the tau protein (45-66 kDa) was in fact not detected in the wild type lenses strongly suggesting that it may be degraded in the wild type lenses. The tau protein was upregulated in α-crystallin knockout lenses in an age-dependent manner, with significant accumulation restricted to the cortical fiber cells of lenses derived from mice older than 6 months of age. Aging lens cortical fiber cells accumulate insoluble proteins, an increase in protein modifications, and a reduction in levels of reduced glutathione, and experience increased oxidative damage [60]. Our data suggest that these changes in the lens may enhance the accumulation of tau in the α-crystallin knockout lenses. Our results contradict a previous report where tau expression was reported in lens as a 36 kDa protein in crude lens soluble and insoluble fractions [36]. Since the molecular mass of tau peptides is normally reported to be 45-66 kDa, the protein at 36 kDa might be a cross-reacting protein in the crude lens preparation. While microtubule motor protein expression has been reported in young rodent lenses [61], it is not known at present whether their expression is age-dependent.

The cortical fibers where tau protein accumulated are particularly interesting because fiber cell changes in this region have been associated with other cataract models including diabetic cataract in rodents [62]. The known ability of tau to enhance microtubule stability suggests that an increase in tau expression may be a response of the lens to the reported increase in instability of the microtubule cytoskeleton in the knockout lenses [42]. Indeed, αA- and αB-crystallin have been shown to enhance the stability of microtubules, and protect tubulin from denaturation [38,42].

One explanation for the observed increase in αB-crystallin in neurodegenerative diseases may be as a failed protective mechanism to suppress tau aggregation and to keep tau proteins in a productive folding pathway. This mechanism may modulate microtubule integrity and accumulation of tau aggregates in the form of neurofibrillary tangles, and αB-crystallin may therefore play a role in the pathogenesis of tau-related diseases [63]. There are at least 6 tau protein isoforms expressed in the brain. In addition to the 45-66 kDa subunits, the αB$^{-/-}$- aged lens cortical fibers also expressed the high molecular weight forms of tau (100 and 200 kDa) suggesting that these might result from crosslinking and aggregation of tau in the lens in the absence of αB-crystallin. It is known that the αA- and αB-crystallin are anti-apoptotic proteins and protect cells from stress-induced death [40,64,65]. The pathogenic

potential of tau and neurofibrillary tangles has been demonstrated by dementia-associated mutations and in transgenic mouse models [66-68]. While αB-crystallin protects against cell death, the increased tau and αB-crystalllin in neuronal pathologies may not be an effective protective mechanism as disease progresses and oxidative stress increases [69].

From our studies, we can propose that the mechanism of tau accumulation as a result of loss of αA- or αB-crystallin chaperones may be an enhanced tendency of tau to misfold and undergo phosphorylation. This hypothesis is lent support by the results of other studies that show that the chaperones HSP70 and HSP90 promote tau solubility and binding to microtubules in the brain, and reduce tau phosphorylation [70]. Furthermore, chaperones are thought to affect cytoskeletal organization and the lack of chaperones or mutations in cytoskeletal proteins or chaperones have been shown to result in inclusion bodies in pathological conditions [11,12,71,72]. Proteasome inhibition stabilizes tau inclusions in oligodendroglial cells [30,73]. Because αB-crystallin is known to target proteins for degradation by the proteasome, another possible mechanism for tau accumulation in α-crystallin gene knockout lenses is that depleting the pool of α-crystallin chaperones impairs the ability of the misfolded tau protein to be targeted to the proteasome [10,17,74]. The increase in tau immunoreactivity observed in the lenses of $\alpha A^{-/-}$-, $\alpha B^{-/-}$-, and $\alpha A/B^{-/-}$- mouse lenses suggests that αA- and αB-crystallin are needed to chaperone tau and assist in its degradation, and in their absence, tau accumulates in the lens.

In summary, the data in this investigation demonstrate the expression of tau transcripts in the lens; describe tau protein accumulation with lens aging in α-crystallin knockout mice; and serve as a basis for characterizing the relationship between tau and α-crystallin function. The current data provide evidence that tau, a microtubule-associated protein whose importance was not apparent from previous analysis in $\alpha A^{-/-}$-, $\alpha B^{-/-}$-, and $\alpha A/B^{-/-}$- mouse lenses, is upregulated when α-crystallin is deleted from the lens. The current work further advances our understanding of the processes that α-crystallin may be involved with and its contribution to lens aging and cataract formation. Moreover, our results suggest that the α-crystallin knockout mice may serve as an important tool to further investigate the relation between tau and αB-crystallin in the brain. Experiments are in progress to determine whether tau is expressed in neuronal disease models and in aged human lenses with and without neurodegeneration.

ACKNOWLEDGEMENTS

The authors thank E. Wawrousek (National Eye Institute, NIH), for providing the α-crystallin gene knockout mice, Belinda McMahan for immunohistochemical analysis, Wandy Beatty for electron microscopic analysis, and Michael Casey in the Molecular Biology Core laboratory for designing primers. This work is supported by the National Eye Institute (NIH) grants R01EY05681 to U.P.A. and the Vision Core grant EY02687, and an unrestricted grant to the Department of Ophthalmology and Visual Sciences from Research to Prevent Blindness, Inc.

REFERENCES

1. Sue Menko A. Lens epithelial cell differentiation. Exp Eye Res 2002; 75:485-90.
2. Bassnett S. Lens organelle degradation. Exp Eye Res 2002; 74:1-6.
3. Bloemendal H, de Jong W, Jaenicke R, Lubsen NH, Slingsby C, Tardieu A. Ageing and vision: structure, stability and function of lens crystallins. Prog Biophys Mol Biol 2004; 86:407-85.
4. Robinson ML, Overbeek PA. Differential expression of alpha A- and alpha B-crystallin during murine ocular development. Invest Ophthalmol Vis Sci 1996; 37:2276-84.
5. Bhat SP, Nagineni CN. alpha B subunit of lens-specific protein alpha-crystallin is present in other ocular and non-ocular tissues. Biochem Biophys Res Commun 1989; 158:319-25.
6. Srinivasan AN, Nagineni CN, Bhat SP. alpha A-crystallin is expressed in non-ocular tissues. J Biol Chem 1992; 267:23337-41.
7. Klemenz R, Frohli E, Steiger RH, Schafer R, Aoyama A. Alpha B-crystallin is a small heat shock protein. Proc Natl Acad Sci U S A 1991; 88:3652-6.
8. Bhat SP. Transparency and non-refractive functions of crystallins—a proposal. Exp Eye Res 2004; 79:809-16.
9. Sax CM, Piatigorsky J. Expression of the alpha-crystallin/small heat-shock protein/molecular chaperone genes in the lens and other tissues. Adv Enzymol Relat Areas Mol Biol 1994; 69:155-201.
10. Boelens WC, Croes Y, de Jong WW. Interaction between alphaB-crystallin and the human 20S proteasomal subunit C8/alpha7. Biochim Biophys Acta 2001; 1544:311-9.
11. Quinlan R. Cytoskeletal competence requires protein chaperones. Prog Mol Subcell Biol 2002; 28:219-33.
12. Quinlan R. Cytoskeletal catastrophe causes brain degeneration. Nat Genet 2001; 27:10-1.
13. Horwitz J. Alpha-crystallin can function as a molecular chaperone. Proc Natl Acad Sci U S A 1992; 89:10449-53.
14. Sun TX, Das BK, Liang JJ. Conformational and functional differences between recombinant human lens alphaA- and alphaB-crystallin. J Biol Chem 1997; 272:6220-5.
15. Van Montfort R, Slingsby C, Vierling E. Structure and function of the small heat shock protein/alpha-crystallin family of molecular chaperones. Adv Protein Chem 2001; 59:105-56.
16. den Engelsman J, Bennink EJ, Doerwald L, Onnekink C, Wunderink L, Andley UP, Kato K, de Jong WW, Boelens WC. Mimicking phosphorylation of the small heat-shock protein alphaB-crystallin recruits the F-box protein FBX4 to nuclear SC35 speckles. Eur J Biochem 2004; 271:4195-203.
17. Lin DI, Barbash O, Kumar KG, Weber JD, Harper JW, Klein-Szanto AJ, Rustgi A, Fuchs SY, Diehl JA. Phosphorylation-dependent ubiquitination of cyclin D1 by the SCF(FBX4-alphaB crystallin) complex. Mol Cell 2006; 24:355-66.
18. Goedert M, Spillantini MG, Jakes R, Rutherford D, Crowther RA. Multiple isoforms of human microtubule-associated protein tau: sequences and localization in neurofibrillary tangles of Alzheimer's disease. Neuron 1989; 3:519-26.
19. Chun W, Johnson GV. The role of tau phosphorylation and cleavage in neuronal cell death. Front Biosci 2007; 12:733-56.
20. Cassimeris L, Spittle C. Regulation of microtubule-associated proteins. Int Rev Cytol 2001; 210:163-226.
21. Goedert M. Tau protein and the neurofibrillary pathology of Alzheimer's disease. Trends Neurosci 1993; 16:460-5.
22. Mandelkow EM, Mandelkow E. Tau in Alzheimer's disease. Trends Cell Biol 1998; 8:425-7.
23. Lee VM, Goedert M, Trojanowski JQ. Neurodegenerative

tauopathies. Annu Rev Neurosci 2001; 24:1121-59.
24. Sobrido MJ, Miller BL, Havlioglu N, Zhukareva V, Jiang Z, Nasreddine ZS, Lee VM, Chow TW, Wilhelmsen KC, Cummings JL, Wu JY, Geschwind DH. Novel tau polymorphisms, tau haplotypes, and splicing in familial and sporadic frontotemporal dementia. Arch Neurol 2003; 60:698-702.
25. Tsuboi Y. Neuropathology of familial tauopathy. Neuropathology 2006; 26:471-4.
26. Buee L, Bussiere T, Buee-Scherrer V, Delacourte A, Hof PR. Tau protein isoforms, phosphorylation and role in neurodegenerative disorders. Brain Res Brain Res Rev 2000; 33:95-130.
27. Muchowski PJ, Wacker JL. Modulation of neurodegeneration by molecular chaperones. Nat Rev Neurosci 2005; 6:11-22.
28. Wilhelmus MM, Otte-Holler I, Wesseling P, de Waal RM, Boelens WC, Verbeek MM. Specific association of small heat shock proteins with the pathological hallmarks of Alzheimer's disease brains. Neuropathol Appl Neurobiol 2006; 32:119-30.
29. Richter-Landsberg C, Bauer NG. Tau-inclusion body formation in oligodendroglia: the role of stress proteins and proteasome inhibition. Int J Dev Neurosci 2004; 22:443-51.
30. Dabir DV, Trojanowski JQ, Richter-Landsberg C, Lee VM, Forman MS. Expression of the small heat-shock protein alphaB-crystallin in tauopathies with glial pathology. Am J Pathol 2004; 164:155-66.
31. Goldstein LE, Muffat JA, Cherny RA, Moir RD, Ericsson MH, Huang X, Mavros C, Coccia JA, Faget KY, Fitch KA, Masters CL, Tanzi RE, Chylack LT Jr, Bush AI. Cytosolic beta-amyloid deposition and supranuclear cataracts in lenses from people with Alzheimer's disease. Lancet 2003; 361:1258-65.
32. Frederikse PH, Garland D, Zigler JS Jr, Piatigorsky J. Oxidative stress increases production of beta-amyloid precursor protein and beta-amyloid (Abeta) in mammalian lenses, and Abeta has toxic effects on lens epithelial cells. J Biol Chem 1996; 271:10169-74.
33. Liang JJ. Interaction between beta-amyloid and lens alphaB-crystallin. FEBS Lett 2000; 484:98-101.
34. Fonte V, Kapulkin V, Taft A, Fluet A, Friedman D, Link CD. Interaction of intracellular beta amyloid peptide with chaperone proteins. Proc Natl Acad Sci U S A 2002; 99:9439-44.
35. Wilhelmus MM, Boelens WC, Otte-Holler I, Kamps B, de Waal RM, Verbeek MM. Small heat shock proteins inhibit amyloid-beta protein aggregation and cerebrovascular amyloid-beta protein toxicity. Brain Res 2006; 1089:67-78.
36. Frederikse PH, Yun E, Kao HT, Zigler JS Jr, Sun Q, Qazi AS. Synapsin and synaptic vesicle protein expression during embryonic and post-natal lens fiber cell differentiation. Mol Vis 2004; 10:794-804.
37. Guzik BW, Goldstein LS. Microtubule-dependent transport in neurons: steps towards an understanding of regulation, function and dysfunction. Curr Opin Cell Biol 2004; 16:443-50.
38. Fujita Y, Ohto E, Katayama E, Atomi Y. alphaB-Crystallin-coated MAP microtubule resists nocodazole and calcium-induced disassembly. J Cell Sci 2004; 117:1719-26.
39. Sakurai T, Fujita Y, Ohto E, Oguro A, Atomi Y. The decrease of the cytoskeleton tubulin follows the decrease of the associating molecular chaperone alphaB-crystallin in unloaded soleus muscle atrophy without stretch. FASEB J 2005; 19:1199-201.
40. Andley UP, Song Z, Wawrousek EF, Bassnett S. The molecular chaperone alphaA-crystallin enhances lens epithelial cell growth and resistance to UVA stress. J Biol Chem 1998; 273:31252-61.
41. Andley UP, Song Z, Wawrousek EF, Brady JP, Bassnett S, Fleming TP. Lens epithelial cells derived from alphaB-crystallin knockout mice demonstrate hyperproliferation and genomic instability. FASEB J 2001; 15:221-229.
42. Xi JH, Bai F, McGaha R, Andley UP. Alpha-crystallin expression affects microtubule assembly and prevents their aggregation. FASEB J 2006; 20:846-57.
43. Xi JH, Bai F, Andley UP. Reduced survival of lens epithelial cells in the alphaA-crystallin-knockout mouse. J Cell Sci 2003; 116:1073-85.
44. Brady JP, Garland D, Duglas-Tabor Y, Robison WG Jr, Groome A, Wawrousek EF. Targeted disruption of the mouse αA-crystallin gene induces cataract and cytoplasmic inclusion bodies containing the small heat shock protein αB-crystallin. Proc Natl Acad Sci U S A 1997; 94:884-9.
45. Brady JP, Garland DL, Green DE, Tamm ER, Giblin FJ, Wawrousek EF. AlphaB-crystallin in lens development and muscle integrity: a gene knockout approach. Invest Ophthalmol Vis Sci 2001; 42:2924-34.
46. Kappe G, Franck E, Verschuure P, Boelens WC, Leunissen JA, de Jong WW. The human genome encodes 10 alpha-crystallin-related small heat shock proteins: HspB1-10. Cell Stress Chaperones 2003; 8:53-61.
47. Goedert M, Jakes R, Vanmechelen E. Monoclonal antibody AT8 recognises tau protein phosphorylated at both serine 202 and threonine 205. Neurosci Lett 1995; 189:167-9.
48. Bussiere T, Hof PR, Mailliot C, Brown CD, Caillet-Boudin ML, Perl DP, Buee L, Delacourte A. Phosphorylated serine422 on tau proteins is a pathological epitope found in several diseases with neurofibrillary degeneration. Acta Neuropathol (Berl) 1999; 97:221-30.
49. Kins S, Crameri A, Evans DR, Hemmings BA, Nitsch RM, Gotz J. Reduced protein phosphatase 2A activity induces hyperphosphorylation and altered compartmentalization of tau in transgenic mice. J Biol Chem 2001; 276:38193-200.
50. LoPresti P, Szuchet S, Papasozomenos SC, Zinkowski RP, Binder LI. Functional implications for the microtubule-associated protein tau: localization in oligodendrocytes. Proc Natl Acad Sci U S A 1995; 92:10369-73.
51. Andley UP, Patel HC, Xi JH, Bai F. Identification of genes responsive to UV-A radiation in human lens epithelial cells using complementary DNA microarrays. Photochem Photobiol 2004; 80:61-71.
52. Vallee RB. A taxol-dependent procedure for the isolation of microtubules and microtubule-associated proteins (MAPs). J Cell Biol 1982; 92:435-42.
53. Bai F, Xi J, Higashikubo R, Andley UP. A comparative analysis of alphaA- and alphaB-crystallin expression during the cell cycle in primary mouse lens epithelial cultures. Exp Eye Res 2004; 79:795-805.
54. Bai F, Xi JH, Wawrousek EF, Fleming TP, Andley UP. Hyperproliferation and p53 status of lens epithelial cells derived from alphaB-crystallin knockout mice. J Biol Chem 2003; 278:36876-86.
55. Mackay DS, Andley UP, Shiels A. Cell death triggered by a novel mutation in the alphaA-crystallin gene underlies autosomal dominant cataract linked to chromosome 21q. Eur J Hum Genet 2003; 11:784-93.
56. Andley UP. Crystallins in the eye: Function and pathology. Prog Retin Eye Res 2007; 26:78-98.
57. Andley UP, Becker B, Hebert JS, Reddan JR, Morrison AR, Pentland AP. Enhanced prostaglandin synthesis after ultraviolet-B exposure modulates DNA synthesis of lens epithelial cells and lowers intraocular pressure in vivo. Invest Ophthalmol Vis Sci 1996; 37:142-53.
58. Girao H, Pereira P, Taylor A, Shang F. Subcellular redistribution

of components of the ubiquitin-proteasome pathway during lens differentiation and maturation. Invest Ophthalmol Vis Sci 2005; 46:1386-92.
59. Awasthi N, Wagner BJ. Suppression of human lens epithelial cell proliferation by proteasome inhibition, a potential defense against posterior capsular opacification. Invest Ophthalmol Vis Sci 2006; 47:4482-9.
60. Giblin FJ. Glutathione: a vital lens antioxidant. J Ocul Pharmacol Ther 2000; 16:121-35.
61. Lo WK, Wen XJ, Zhou CJ. Microtubule configuration and membranous vesicle transport in elongating fiber cells of the rat lens. Exp Eye Res 2003; 77:615-26.
62. Tunstall MJ, Eckert R, Donaldson P, Kistler J. Localised fibre cell swelling characteristic of diabetic cataract can be induced in normal rat lens using the chloride channel blocker 5-nitro-2-(3-phenylpropylamino) benzoic acid. Ophthalmic Res 1999; 31:317-20.
63. Feinstein SC, Wilson L. Inability of tau to properly regulate neuronal microtubule dynamics: a loss-of-function mechanism by which tau might mediate neuronal cell death. Biochim Biophys Acta 2005; 1739:268-79.
64. Andley UP, Song Z, Wawrousek EF, Fleming TP, Bassnett S. Differential protective activity of alphaA- and alphaB-crystallin in lens epithelial cells. J Biol Chem 2000; 275:36823-31.
65. Kamradt MC, Chen F, Sam S, Cryns VL. The small heat shock protein alpha B-crystallin negatively regulates apoptosis during myogenic differentiation by inhibiting caspase-3 activation. J Biol Chem 2002; 277:38731-6.
66. DeTure M, Ko LW, Yen S, Nacharaju P, Easson C, Lewis J, van Slegtenhorst M, Hutton M, Yen SH. Missense tau mutations identified in FTDP-17 have a small effect on tau-microtubule interactions. Brain Res 2000; 853:5-14.
67. Lewis J, McGowan E, Rockwood J, Melrose H, Nacharaju P, Van Slegtenhorst M, Gwinn-Hardy K, Paul Murphy M, Baker M, Yu X, Duff K, Hardy J, Corral A, Lin WL, Yen SH, Dickson DW, Davies P, Hutton M. Neurofibrillary tangles, amyotrophy and progressive motor disturbance in mice expressing mutant (P301L) tau protein. Nat Genet 2000; 25:402-5. Erratum in: Nat Genet 2000; 26:127.
68. Hutton M, Lewis J, Dickson D, Yen SH, McGowan E. Analysis of tauopathies with transgenic mice. Trends Mol Med 2001; 7:467-70.
69. Newman SF, Sultana R, Perluigi M, Coccia R, Cai J, Pierce WM, Klein JB, Turner DM, Butterfield DA. An increase in S-glutathionylated proteins in the Alzheimer's disease inferior parietal lobule, a proteomics approach. J Neurosci Res 2007; 85:1506-14.
70. Dou F, Netzer WJ, Tanemura K, Li F, Hartl FU, Takashima A, Gouras GK, Greengard P, Xu H. Chaperones increase association of tau protein with microtubules. Proc Natl Acad Sci U S A 2003; 100:721-6.
71. Clark JI, Matsushima H, David LL, Clark JM. Lens cytoskeleton and transparency: a model. Eye 1999; 13:417-24.
72. Clark JI, Muchowski PJ. Small heat-shock proteins and their potential role in human disease. Curr Opin Struct Biol 2000; 10:52-9.
73. Goldbaum O, Oppermann M, Handschuh M, Dabir D, Zhang B, Forman MS, Trojanowski JQ, Lee VM, Richter-Landsberg C. Proteasome inhibition stabilizes tau inclusions in oligodendroglial cells that occur after treatment with okadaic acid. J Neurosci 2003; 23:8872-80.
74. den Engelsman J, Keijsers V, de Jong WW, Boelens WC. The small heat-shock protein alpha B-crystallin promotes FBX4-dependent ubiquitination. J Biol Chem 2003; 278:4699-704.

The print version of this article was created on 6 Sep 2007. This reflects all typographical corrections and errata to the article through that date. Details of any changes may be found in the online version of the article.